JMEPEG (2015) 24:1065–1071
DOI: 10.1007/s11665-014-1336-6

1059-9495/$19.00

Welding of 316L Austenitic Stainless Steel with Activated Tungsten Inert Gas Process

E. Ahmadi and A.R. Ebrahimi

(Submitted June 3, 2014; in revised form September 21, 2014; published online December 30, 2014)

The use of activating flux in TIG welding process is one of the most notable techniques which are developed recently. This technique, known as A-TIG welding, increases the penetration depth and improves the productivity of the TIG welding. In the present study, four oxide fluxes (SiO_2, TiO_2, Cr_2O_3, and CaO) were used to investigate the effect of activating flux on the depth/width ratio and mechanical property of 316L austenitic stainless steel. The effect of coating density of activating flux on the weld pool shape and oxygen content in the weld after the welding process was studied systematically. Experimental results indicated that the maximum depth/width ratio of stainless steel activated TIG weld was obtained when the coating density was 2.6, 1.3, 2, and 7.8 mg/cm^2 for SiO_2, TiO_2, Cr_2O_3, and CaO, respectively. The certain range of oxygen content dissolved in the weld, led to a significant increase in the penetration capability of TIG welds. TIG welding with active fluxes can increase the delta-ferrite content and improves the mechanical strength of the welded joint.

Keywords activating flux, coating density, depth/width ratio, TIG welding

1. Introduction

In the family of stainless steels, austenitic stainless steels have attracted great attention due to excellent properties such as ductility, high strength, and corrosion resistance. More than 50% of the total volume of wrought stainless steel products is made from austenitic stainless steel (Ref 1). The joining process of these stainless steels are often done by the shielded metal arc welding (SMAW), the metal inert gas welding (GMAW, MIG), and the tungsten inert gas welding (GTAW, TIG). The TIG welding process is a popular process in this area where a high degree of quality and accuracy is required. Moreover, TIG welding is more preferable than SMAW and MIG process because of the lower heat input. The lower heat input results in faster cooling rates which helps overcoming the problem of sensitization, thus leading to a remedy to the problems of intergranular corrosion (IGC) and intergranular stress corrosion cracking (Ref 2). However, this process has relatively shallow penetration capability and low productivity, particularly in single-pass welding operations in the welding of large components, compared to other welding processes.

In order to improve the TIG penetration depth, many studies have been conducted since 1995. Experimental works led to the innovation of processes such as activating tungsten inert gas (A-TIG) (Ref 3), magnetic tungsten inert gas (M-TIG) (Ref 4), keyhole tungsten inert gas (K-TIG) (Ref 5), and Ultrasonic Tungsten Inert Gas (U-TIG) (Ref 6). Among these methods, A-TIG process has gained considerable attention due to its low cost and ease of operation. This process was first proposed by Paton Electric Welding Institute in the 1960s and characterized by applying a thin layer of an activating flux on the surface of the base metal. Activating fluxes increase weld depth penetration with the changing behavior of arc plasma column and weld pool fluid flow of TIG welding.

Although the A-TIG technique is used in various industries, such as United States Navy Joining Center, nuclear power plant of Japan, etc., there is still no common understanding on the explanation of mechanism of increasing A-TIG welding penetration depth. In the latest third century four proposed mechanisms were proposed. The first mechanism was proposed by Savitskii and Leskov in 1980, and was based on the idea that the flux as a surface active agent (surfactant) reduces the surface tension of the molten weld pool (Ref 7). Reduction of surface tension results in formation of a small cavity at the weld pool surface which supports the arc pressure. This mechanism is called the TIG keyhole mode. The second mechanism was proposed by Heiple and Ropper in 1982 and was based on the Marangoni effect (Ref 8). This theory says that the activating fluxes change the gradient of the surface tension from negative to positive which causes the molten metal to flow in the opposite direction toward the center. The validity of this theory was confirmed by following the motion of the tungsten particle in TIG and A-TIG weld pool by x-ray transmission method (Ref 9). A third mechanism was explained through the constriction of the welding arc because of the vaporized flux molecules, by Howse and Lucas in 2000 (Ref 10).The last proposed mechanism until now, was expressed by the Lowke and co-workers in 2004. It is considered that activating flux behaves as an electrical insulator and increases the weld depth penetration (insulation mode) (Ref 11). Schematic diagram of the four mechanisms are shown in Fig. 1. In order to evaluate the effect of activating flux components on the TIG welding process, the A-TIG welding of 316L austenitic stainless steels

E. Ahmadi, Materials Engineering Department, Sahand University of Technology, Tabriz, Iran; and **A.R. Ebrahimi**, Mining and Metallurgical Engineering Department, Amirkabir University of Technology, Tehran, Iran. Contact e-mail: e.ahmadiii@gmail.com.

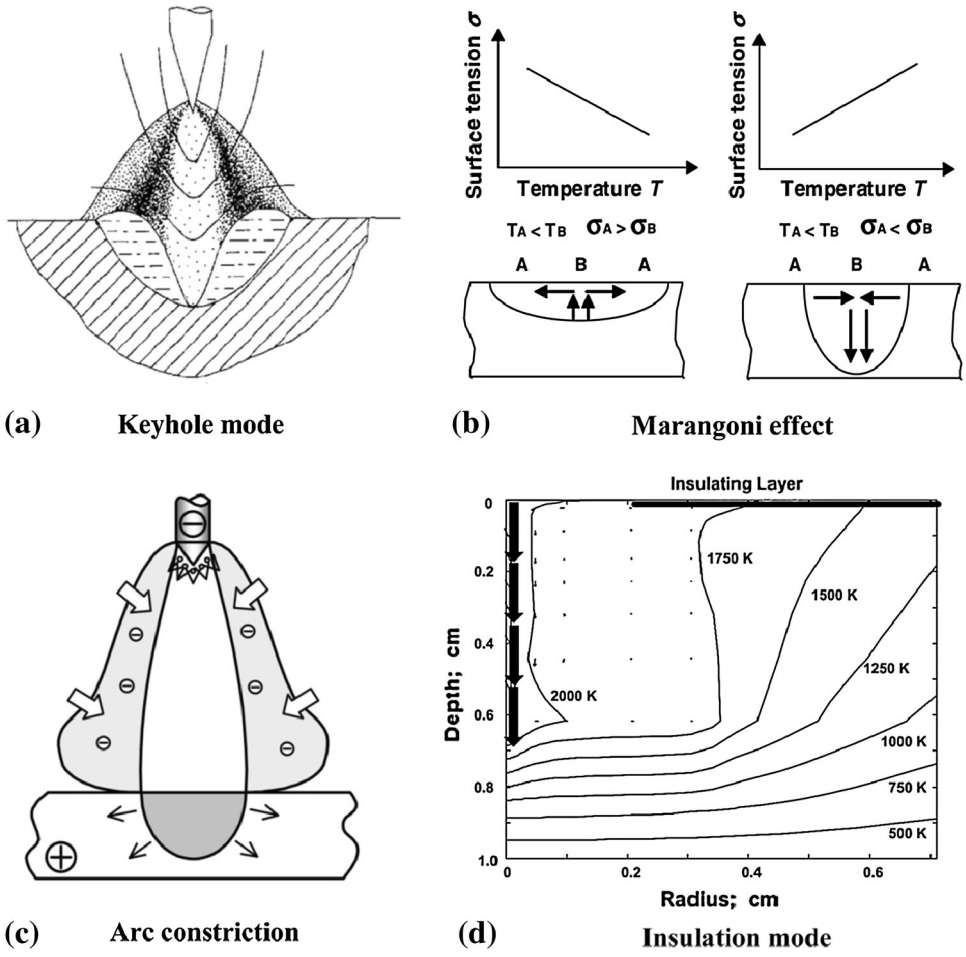

Fig. 1 Schematic diagram of four proposed mechanisms (Ref 7, 8, 10, 11)

with four different kinds of oxide fluxes (SiO_2, TiO_2, Cr_2O_3, and CaO) was studied in the present work.

2. Experimental Procedure

316L austenitic stainless steel alloy wrought plates with dimensions of 150 mm × 150 mm × 9 mm were selected for the welding experiments, with the average composition of 0.025%C, 0.48%Si, 1.26%Mn, 10.2%Ni, 17.7%Cr, 0.032%P, 0.002%S, 0.0021%O and the rest of Fe. Before welding, surfaces of the plates were ground with 400-grit flexible abrasive paper and chemically cleaned with acetone to eliminate surface impurities. Four kinds of oxide powders (SiO_2, TiO_2, Cr_2O_3, and CaO) were used as activating fluxes in the experiment, with about 40-60 μm particle size. The flux was mixed with acetone and painted onto the surface of the workpiece prior to welding. Evaporation of the acetone helped a layer of flux adhere to the surface. GTA bead-on-plate welds were used with direct current electrode negative and a mechanized control system in which the workpieces were moves at the adjusted speed. The welding parameters are listed in Table 1. In order to observe and record images of the molten pool and weld arc and analyze the relationship between penetration increase and arc profile, a charge coupled device (CCD) camera system was used during welding processes, as Fig. 2 schematically illustrates.

Table 1 Welding parameters

Parameters	Value
Electrode type	DCEN, W-2% ThO_2
Diameter of electrode	3.2 mm
Vertex angle of electrode	60°
Welding current	150 A
Welding speed	150 mm/min
Arc length	3 mm
Shielding gas	Pure argon
Gas flowrate	12 L/min

In this experiment, ferrite number (FN) in the weld metal and base material was measured using a calibrated magnetic instrument (ferritoscope). This device detects phases such as ferrite by their magnetic susceptibility, which differs from that of the paramagnetic austenite. To minimize measurement errors resulting from inhomogeneity in the weld metals, the average value of seven measurements from various locations along the as-welded surface was calculated. Oxygen analysis was carried out on a LECO TC-436 apparatus. In order to examine the mechanical properties, tensile properties of A-TIG stainless steel welds, including longitudinal tensile tests were used. The configuration and size of the tensile specimens were in accordance with ASTM E8.

3. Results and Discussion

3.1 Weld Morphology

Several experiments with different quantity of flux from 0.1 to 8 mg/cm^2 were carried out to study the effects of coating density of flux on the weld penetration and determine the optimum quantity of flux in activated GTA weld. The weld penetration depth and weld bead width were plotted versus different quantity of fluxes in Fig. 3. It is clear that all the fluxes significantly increased the penetration depth in a certain range of coating density of fluxes, compared with the penetration depth of conventional TIG (zero coating density). However, with increasing coating density of fluxes, each flux showed a different effect on the weld morphology. Except CaO, all the other fluxes had a similar effect on the weld depth penetration, therefore penetration considerably increased initially and then decreased with increasing flux coating density. The maximum penetration was achieved in the 2.4, 2.1, and 3.6 mg/cm^2 coating density of SiO_2, Cr_2O_3, and TiO_2 fluxes, respectively. For CaO flux, weld penetration increased steadily with increasing flux quantity up to 7.8 mg/cm^2. Moreover, it is obvious from the Fig. 3 that the SiO_2 and Cr_2O_3 fluxes reduce the bead width of weld only in a limited range of coating density of flux compared with conventional TIG, while the CaO and TiO_2 fluxes decreased the bead width initially and reached a constant value with increase in flux quantity. Therefore, in order to achieve an optimal flux quantity, the depth to width ratio factor which plays an important role in determining the quality of joint was calculated based on the weld geometry sizes (Fig. 3) and plotted versus the coating density of fluxes as shown in Fig. 4.

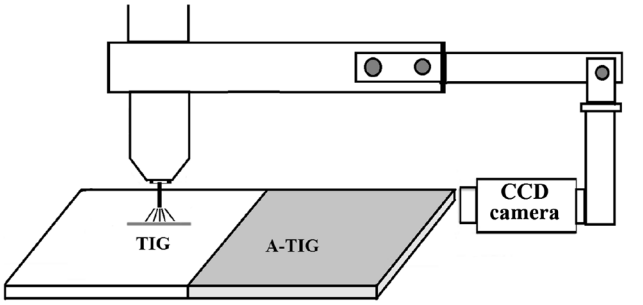

Fig. 2 Schematic representation of CCD camera

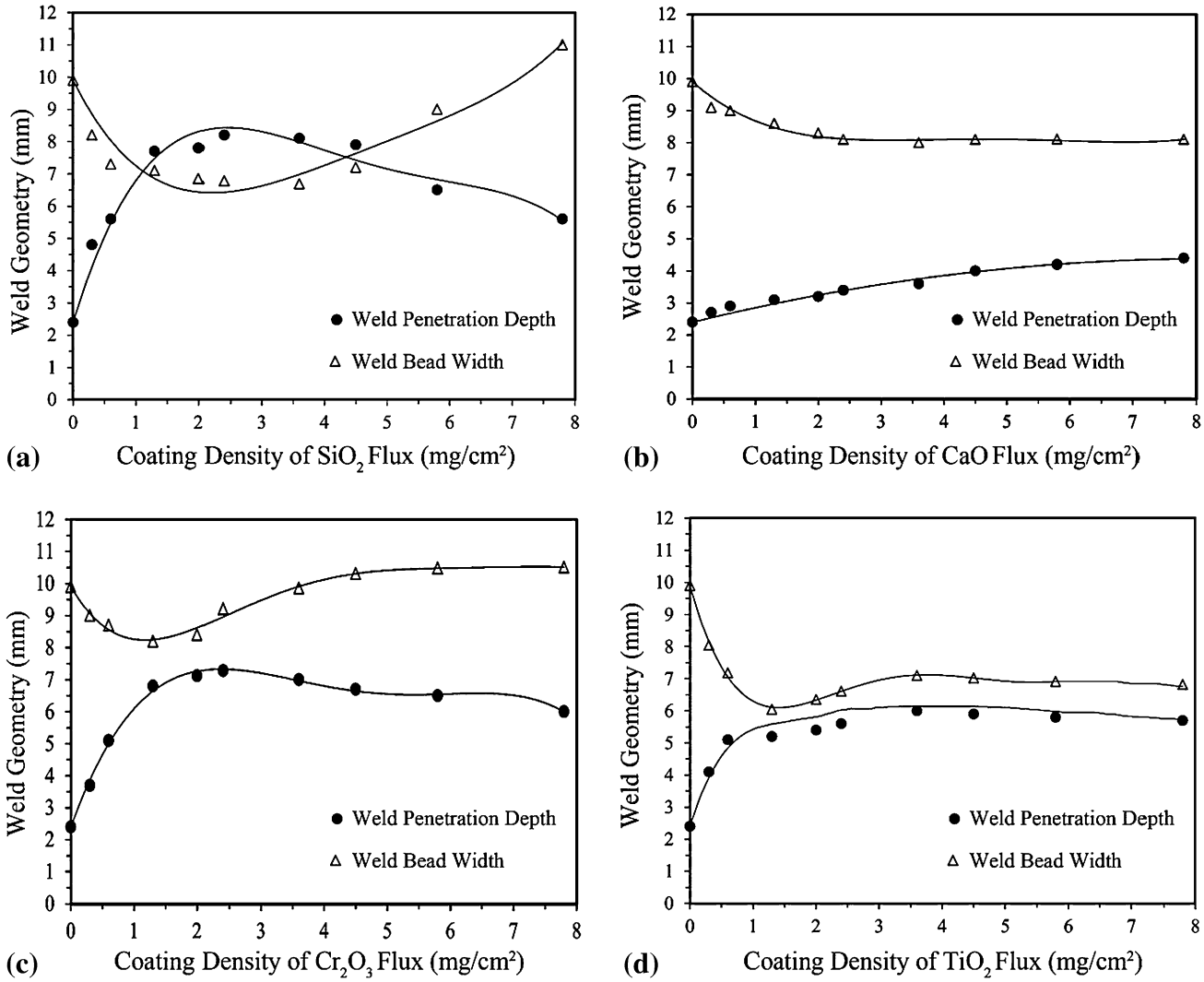

Fig. 3 Effect of flux quantity on penetration depth and bead width of weld

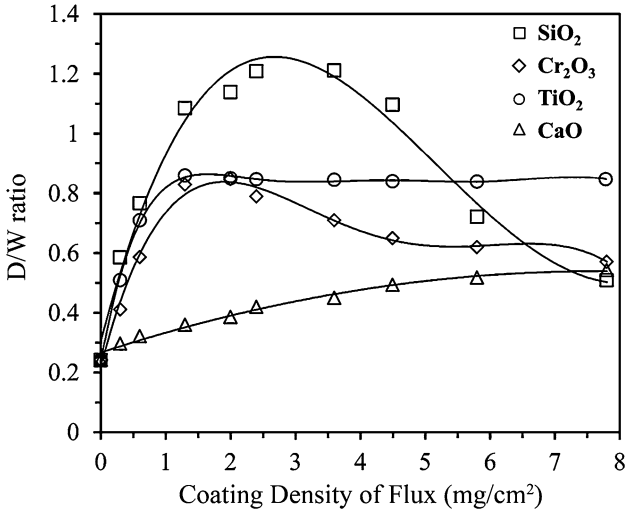

Fig. 4 Effect of flux quantity on depth to width ratio

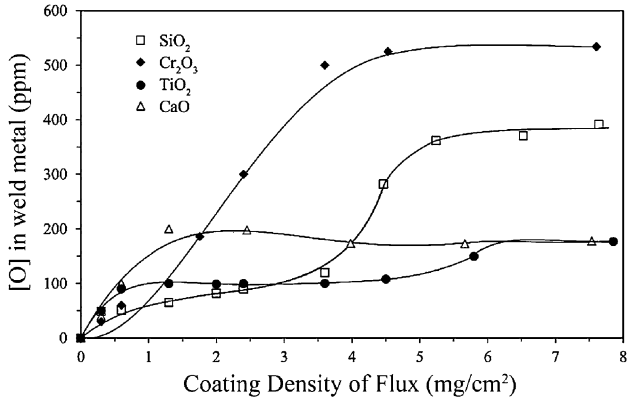

Fig. 5 Effect of flux quantity on the weld metal oxygen content

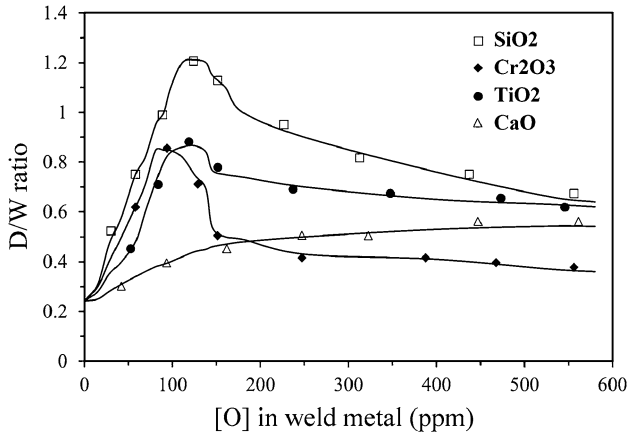

Fig. 6 Effect of oxygen content in weld on the weld/width ratio of weldments

This has been proven that the fluid flow in the weld pool is under the influence of the forces of buoyancy, Lorenz, Marangoni, and arc pressure. Among them, Marangoni force is predominant under normal welding condition and has main effect on the weld shape. The Marangoni flow is a fluid flow from a region of low surface tension to high surface tension due to the surface tension gradient caused by the temperature difference, composition difference, and electric potential difference along a surface of weld pool (Ref 12). Therefore, Marangoni forces induce an outward flow along the surface of the pool (from center to edges) and results in formation of a wide and shallow weld pool. The surface tension of many alloys decreases as the temperature increases ($\partial\gamma/\partial T < 0$) (Ref 13-15). Many research results have shown that in the presence of a certain amount of oxygen in weld pool, Marangoni flow turns inward (from edges to center) and forms a narrow and deep weld pool. This is because, the oxygen acts as a surfactant agent for pure iron and stainless steel, which makes the temperature coefficient of the surface tension change from negative to positive ($\partial\gamma/\partial T > 0$) (Ref 16-18). Taimatsu et al. have reported that for pure liquid iron, the temperature coefficient of the surface tension is positive in the oxygen content range of 150-350 ppm and out of this range, the temperature coefficient of the surface tension becomes zero or negative.

Analysis of oxygen content in weld was carried out after welding and plotted versus flux quantity and D/W ratio in Fig. 5 and 6, respectively. Figure 5 illustrates that the weld metal oxygen content suddenly increases with the activating fluxes usage due to decomposition of oxide powder under plasma temperature. Oxygen content in the weld metal increased in the order of TiO_2, CaO, SiO_2, and Cr_2O_3. This result can be justified by considering the thermodynamic stability of oxide fluxes. According to Ellingham diagram, which plots the Gibbs free energy change (ΔG) for each oxidation reaction as a function of temperature, oxides of titanium and chromium have respectively high and low degree of thermodynamic stability. Moreover, the weld depth to width ratio suddenly increased from 0.242 to 0.46-1.12 when the oxygen content in weld was in the range of 75-150 ppm as presented in Fig. 6. It is clear that except the CaO flux, the maximum depths of penetration for other fluxes are in the range of 1.5 to 3 mg/cm^2. The conclusion by Pollard (Ref 19) showed that Calcium is a reactive element that tends to cause poor penetration by reacting with free oxygen in the molten weld pool. For this reason, oxygen content in weld metal slowly increased up to 150 ppm with increase in the quantity of CaO flux, and weld penetration depth reached to maximum value. Therefore, the results presented in Fig. 3-6 shows that the oxygen in 316L stainless steel weld pool has the similar effect with pure liquid iron. Therefore, in the certain range of oxygen content, the weld penetration and D/W ratio increased while the weld metal width decreased. This is can be attributed to the change of negative temperature coefficient of the surface tension of conventional TIG to positive temperature coefficient of the surface tension of A-TIG. Also, this sudden increase in the D/W ration can be explained by the arc contraction theories.

The optical macrographs, cross sections of TIG welds with and without the optimal flux quantity in 316L stainless steel at the same welding condition are shown in Fig. 7. It can be seen that, activating fluxes greatly increased the weld penetration and distinctly changed the weld shape profile. The SiO_2 flux showed a greater ability to increase the weld penetration and D/W ratio than other fluxes. This happens due to the reason that, the silicon reduces the viscosity of weld pool, therefore if a downward flow pattern existed (reverse Marangoni flow), the flow velocity increased and hence weld penetration increases (Ref 20). The cross-sectional views of arc plasma column with geometric characteristics of weld metal are also shown in Fig. 7. It was

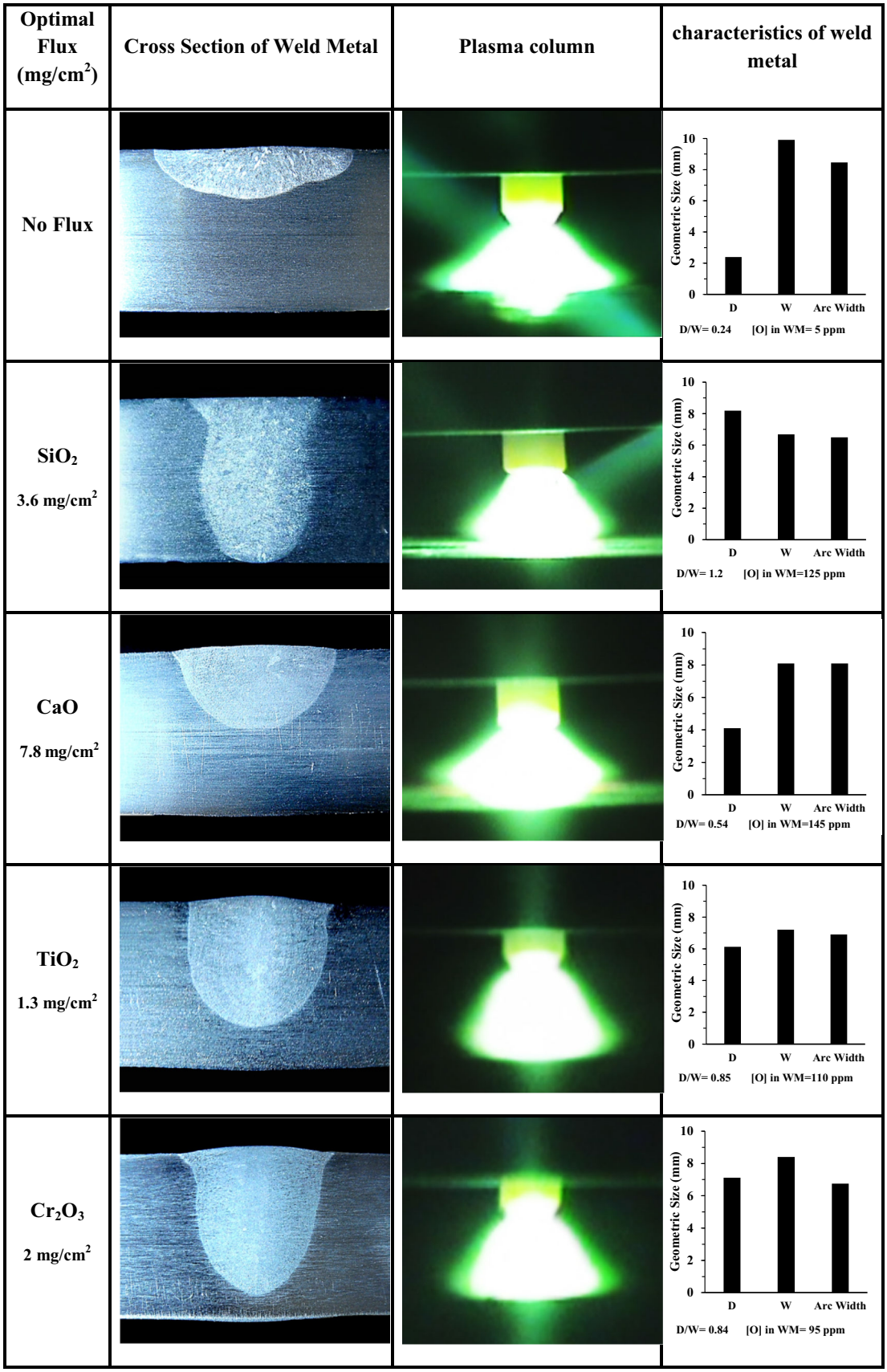

Fig. 7 Weld characterizes without and with optimal activating fluxes

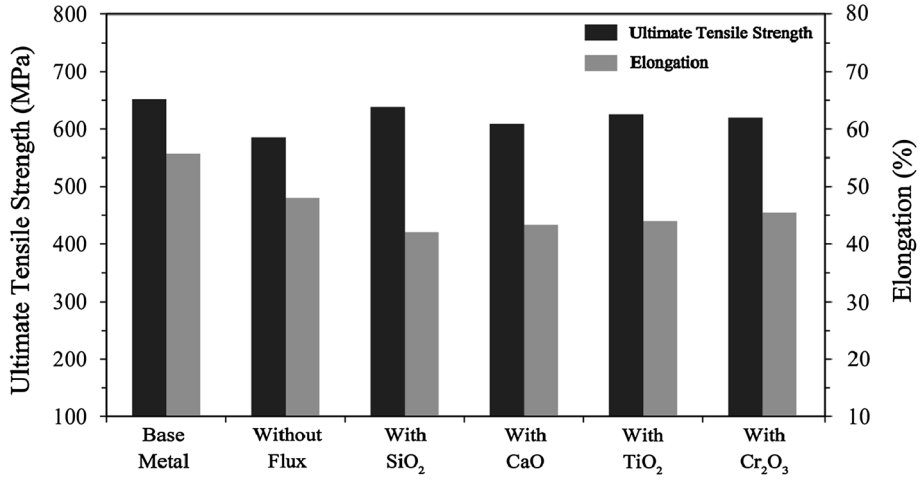

Fig. 8 Effect of activating fluxes on mechanical properties

Table 2 Effect of activating fluxes on ferrite content (FN)

Alloy	Base Metal	Without Flux	SiO_2	CaO	TiO_2	Cr_2O_3
Ferrite content (FN)	0.87	6.5	7.6	6.8	7.3	7.7

observed that the activating flux influences the shape of plasma column. The diameter of the plasma column contracted with activating TIG welding compared with the conventional TIG at the same current level. It is proposed that due to extremely high temperature of the arc, the activating fluxes will evaporate. The evaporated molecules of fluxes with electron capture in the outer region of the arc, lead to the arc constriction (Ref 21).

In other words, in the central region of arc, the arc temperature is high enough to completely dissociate any molecules of flux and shielding gas and ionize their atoms. So, ionizing the atoms and molecules produces electrons and positive ions. In the peripheral region of arc, molecules and atoms of dissolved flux exist and to which electrons attach and form negatively charged particles. For this reason, number of electrons in peripheral region which are the major charge carriers reduces and diameter of arc plasma column constricts (Ref 22). Figure 7 clearly demonstrates that the SiO_2 flux has a significant effect on the contraction of the plasma column diameter. This may be due to the higher resistivity of nonmetal silicon dioxide powder than other powders. In this case, the formation of electrically conductive channel between electrode and SiO_2 flux surface is very difficult, and the conductive channel can only be formed on the small part of metal surface where the SiO_2 flux film is evaporated by arc energy. As a result, the arc plasma is formed with a smaller diameter.

3.2 Mechanical Properties

Figure 8 presents the experimental results for the transverse tensile test of the TIG weldment with and without flux. The mechanical properties of 316L base metal which is a wrought alloy, was better than as-welded alloys due to the work hardening. It can be seen from Fig. 8 that all the activating fluxes greatly increased the tensile strength of weld compared to conventional TIG weld without flux. The ultimate tensile strength of weld obtained with SiO_2 flux was the highest among

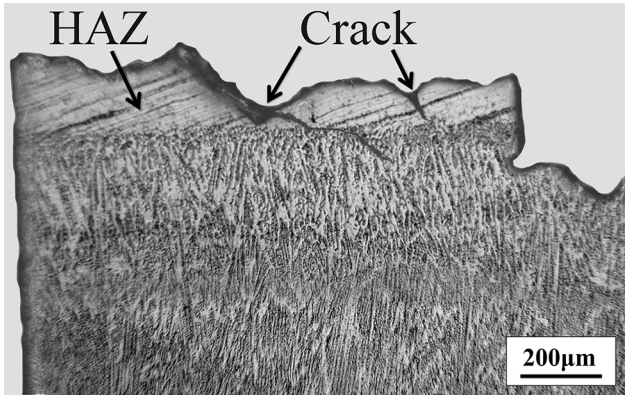

Fig. 9 Optical micrograph of the etched cross section of a failed weld with SiO_2 flux in a solution of 10 g $CuSO_4$ + 50 ml HCl + 50 ml H_2O

other fluxes which is close to the base metal. Improvement of mechanical properties with activating fluxes can be attributed to increase of delta-ferrite in weld metal (Table 2). The results indicated that increase in the delta-ferrite content caused increase in the tensile strength, while the elongation slightly decreased. This is because most of the weld metals of austenitic stainless steel solidified in delta-ferrite phase (Ref 23). The delta-ferrite has a body-centered cubic (BCC) crystal structure, while the austenite has a cubic face-centered (FCC) crystal structure. As BCC structure has a higher mechanical strength compared to FCC structure, usage of activating flux in TIG welding leads to beneficial effects in increasing the strength of 316L stainless steel welds.

During the tensile tests, all the weldments showed a similar behavior and failed in the heat-affected zone. Optical microscopic examination of cross section taken from fracture areas of 316L stainless steel TIG weldment with SiO_2 flux is shown in

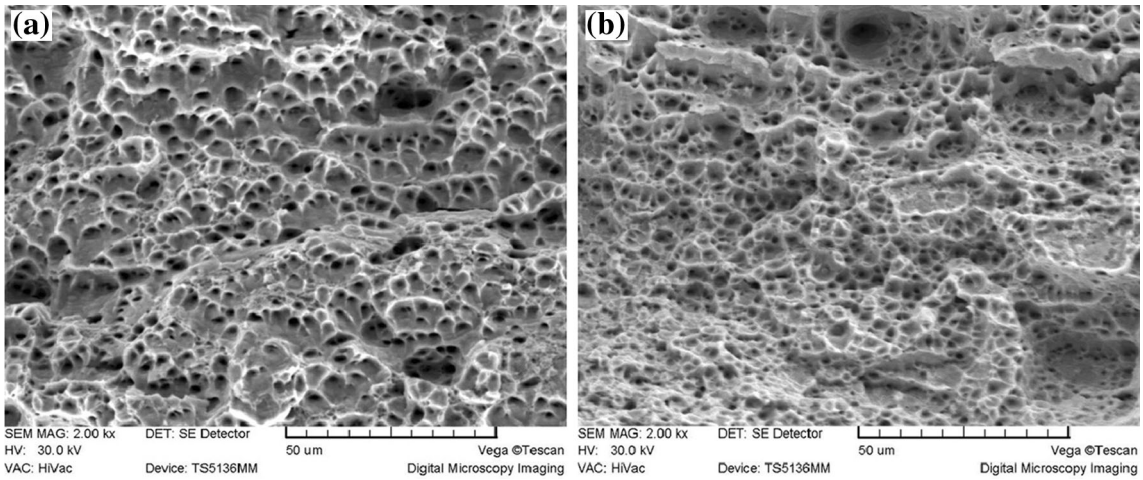

Fig. 10 Scanning electron micrograph (SEM) of fracture surface, (a) without flux (b) with SiO_2 flux

Fig. 9. It is clearly evident from Fig. 9 that cracks propagate along coarse structure of heat-affected zone. The analysis of the fracture surfaces of TIG weldment with and without SiO_2 flux is shown in Fig. 10. Dimple structures are observed at the fracture surfaces, indicating of ductile fracture mechanism for both TIG weldments with and without flux.

4. Conclusions

(1) When using a certain coating density of activating fluxes, the weld penetration and D/W ratio increased while the weld metal width decreased. Among the fluxes, the SiO_2 flux had a significant effect on enhancing the weld penetration in A-TIG.
(2) The oxygen is an active element for 316L stainless steel, therefore in the range of 70-150 ppm in weld pool, the weld depth/width ratio suddenly increased and out of this range no effect was observed on the enhanced penetration depth.
(3) Activating flux can constrict the plasma column diameter compared with the conventional TIG welding arc at the same current level.
(4) A-TIG welding can increase ultimate tensile strength of weldments because of increasing the retained delta-ferrite content of stainless steel welds.

References

1. C.R. Brinkman and H.W. Garvin, *Properties of Austenitic Stainless Steels and Their Weld Metals (Influence of Slight Chemistry Variations)*, ASTM International, Novelty, OH, 1979
2. H.S. Khatak and B. Raj, *Corrosion of Austenitic Stainless Steels, Mechanism, Mitigation and Monitoring*, Woodhead Publishing Series in Metals and Surface Engineering Elsevier, New York, 2002
3. T. Paskell, C. Lundin, and H. Castner, GTAW Flux Increases Weld Joint Penetration, *Weld. J.*, 1997, **76**, p 57–62
4. K. Nomuraa, Y. Oginob, and Y. Hirataa, Shape Control of TIG Arc Plasma by Cusp-Type Magnetic Field with Permanent Magnet, *Weld. Int.*, 2012, **26**, p 759–764
5. B. Jarvis and N. Ahmed, Development of Keyhole Mode Gas Tungsten Arc Welding Process, *Sci. Technol. Weld. Join.*, 2000, **5**, p 1–7
6. Q.J. Sun, S.B. Lin, C.L. Yang, and G.Q. Zhao, Penetration Increase of AISI, 304 Using Ultrasonic Assisted Tungsten Inert Gas Welding, *Sci. Technol. Weld. Join.*, 2009, **14**, p 765–767
7. M. Savitskii and G.I. Leskov, Mechanizm vliyamia dzlektrootrida tepvnykh zpementov na proplavlauchyu sposovnosti luqi s volifra-moym katodm Avtom, *Svarka*, 1980, **9**, p 17–22
8. C. Heiple and J. Roper, Mechanism for Minor Element Effect on GTA Fusion Zone Geometry, *Weld. J.*, 1982, **61**, p 97–108
9. C. Dong and S. Katayama, Basic Understanding of A-TIG Welding Process, *The 57th Annual Assembly of the International Institute of Welding*, 2004, (Osaka), IIW Doc.212-1055-042004
10. D.S. Howse and W. Lucas, Investigation into Arc Constriction by Active Fuxes for Tungsten Inert Gas Welding, *Sci. Technol. Weld. Join.*, 2000, **5**, p 189–193
11. J.J. Lowke, M. Tanake, and M. Ushio, Insulation Effects of flux Layer in Producing Greater Weld Depth, *The 57th Annual Assembly of International Institute of Welding*, 2004 (Osaka), IIW Doc.212-1053-04, 2004
12. Y.L. Xu, Z.B. Dong, Y.H. Wei, and C.L. Yang, Marangoni Convection and Weld Shape Variation in A-TIG Welding Process, *Theoret. Appl. Fract. Mech.*, 2007, **48**, p 178–186
13. K.C. Mills, B.J. Keene, R.F. Brooks, and A. Shirali, Marangoni Effects in Welding, *Philos. Trans. R. Soc. A*, 1998, **356**, p 911–925
14. M.G. Velarde and RKh Zeytourian, *Interfacial Phenomena and the Marangoni Effect*, Springer, NewYork, 2003, p 226–254
15. Sh Lu, H. Fujii, and K. Nogi, Marangoni Convection and Weld Shape Variations in He-CO_2 Shielded Gas Tungsten Arc Welding on SUS304 Stainless Steel, *J. Mater. Sci.*, 2008, **43**, p 4583–4591
16. D.K. Aidun and S.A. Martin, Effect of Sulphur and Oxygen on Weld Penetration of High-Purity Austenitic Stainless Steel, *J. Mater. Eng. Perform.*, 1997, **6**, p 496–502
17. P. Sahoo, T. DebRoy, and M.T. McNallan, Surface Tension of Binary Metal Surface Active Solute Systems Under Conditions Relevant to Welding Metallurgy, *Metall. Mater. Trans. B*, 1988, **19**, p 483–491
18. H. Taimatsu, K. Nogi, and K. Ogino, Surface Tension of Liquid Fe-O Alloy, *J. High Temp. Soc.*, 1992, **18**, p 14–19
19. B. Pollard, The Effects of Minor Elements on the Welding Characteristics of Stainless Steel, *Weld. J.*, 1988, **67**, p 202–213
20. P.J. Modenesi, E. Aquio, R.A. Ario, and I.M. Pereira, TIG Welding with Single-Component Fluxes, *J. Mater. Process. Technol.*, 2000, **99**, p 260–265
21. M.L. Lin and T.W. Eagar, Influence of Arc Pressure on Weld Pool Geometry, *Welding Journal*, 1985, **64**, p 163–169
22. V.S. Mechev, Mechanism of Contraction of the Welding Arc in the Presence of Electronegative Particles, *Weld. Int.*, 1993, **7**, p 154–156
23. A.F. Padilha, C.F. Tavares, and M.A. Martorano, Delta Ferrite Formation in Austenitic Stainless Steel Castings, *Mater. Sci. Forum*, 2013, **730-732**, p 733–738